

Compartmentalization and Ca^{2+} Buffering Are Essential for Prevention of Light-Induced Retinal Degeneration

Shirley Weiss,¹ Elkana Kohn,¹ Daniela Dadon,¹ Ben Katz,¹ Maximilian Peters,¹ Mario Lebendiker,² Mickey Kosloff,³ Nansi Jo Colley,⁴ and Baruch Minke¹

¹Department of Medical Neurobiology, Institute for Medical Research Israel-Canada (IMRIC) and the Edmond and Lily Safra Center for Brain Sciences (ELSC), Faculty of Medicine, the Hebrew University, Jerusalem 91120, Israel, ²Unit for Structural Biology, Silverman Institute for Life Sciences, The Hebrew University, Jerusalem 91904, Israel, ³Department of Biology, University of Haifa, Haifa 31905, Israel, and ⁴Department of Ophthalmology & Visual Sciences, Department of Genetics, UW Eye Research Institute, University of Wisconsin, Madison, Wisconsin 53792

Fly photoreceptors are polarized cells, each of which has an extended interface between its cell body and the light-signaling compartment, the rhabdomere. Upon intense illumination, rhabdomeric calcium concentration reaches millimolar levels that would be toxic if Ca^{2+} diffusion between the rhabdomere and cell body was not robustly attenuated. Yet, it is not clear how such effective attenuation is obtained. Here we show that Ca^{2+} homeostasis in the photoreceptor cell relies on the protein calphotin. This unique protein functions as an immobile Ca^{2+} buffer localized along the base of the rhabdomere, separating the signaling compartment from the cell body. Generation and analyses of transgenic *Drosophila* strains, in which calphotin-expression levels were reduced in a graded manner, showed that moderately reduced calphotin expression impaired Ca^{2+} homeostasis while calphotin elimination resulted in severe light-dependent photoreceptor degeneration. Electron microscopy, electrophysiology, and optical methods revealed that the degeneration was rescued by prevention of Ca^{2+} overload via overexpression of CalX, the $\text{Na}^+ - \text{Ca}^{2+}$ exchanger. In addition, Ca^{2+} -imaging experiments showed that reduced calphotin levels resulted in abnormally fast kinetics of Ca^{2+} elevation in photoreceptor cells. Together, the data suggest that calphotin functions as a Ca^{2+} buffer; a possibility that we directly demonstrate by expressing calphotin in a heterologous expression system. We propose that calphotin-mediated compartmentalization and Ca^{2+} buffering constitute an effective strategy to protect cells from Ca^{2+} overload and light-induced degeneration.

Introduction

Many neurons localize Ca^{2+} -permeable channels into a small volume, resulting in local but sizable changes in Ca^{2+} concentration ($[\text{Ca}^{2+}]$) (Augustine and Neher, 1992; Koch and Zador, 1993; Lenzi and Roberts, 1994). Fly photoreceptors exemplify this strategy by means of a specialized signaling compartment, the rhabdomere. The transduction machinery is housed in the rhabdomere, while the nucleus and cellular organelles reside in the cell body (Hardie and Raghu, 2001; Katz and Minke, 2009). Upon intense illumination, Ca^{2+} selective transient receptor po-

tential (TRP) channels (Hardie and Minke, 1992; Peretz et al., 1994a), located in the rhabdomeric microvilli (Huber et al., 1996; Tsunoda et al., 1997), are robustly activated, causing rhabdomeric $[\text{Ca}^{2+}]$ to undergo a very rapid (~ 20 ms) and large ($> 500 \mu\text{M}$) transient increase. In contrast, $[\text{Ca}^{2+}]$ in the cell body rises at a lower rate and reaches lower concentration ($\sim 10 \mu\text{M}$) (Oberwinkler and Stavenga, 2000b). Ca^{2+} imaging in the *Calliphora* fly (Oberwinkler and Stavenga, 2000b) and studies of *Drosophila* mutants with a reduced $\text{Na}^+ - \text{Ca}^{2+}$ exchanger expression (CalX) (Wang et al., 2005) revealed that CalX localization is adjacent to the TRP channels within the microvilli. This colocalization provides efficient Ca^{2+} extrusion, which is functionally important for both the visual response and for cell survival. Yet, it is unknown how Ca^{2+} diffusion to the cell body is attenuated and how relatively low $[\text{Ca}^{2+}]$ is maintained in the cell body during intense illumination.

Calphotin (Cpn), an unusual protein discovered by Benzer and colleagues (Martin et al., 1993), is restricted to a defined cytoplasmic region adjacent to the base of the rhabdomere (Martin et al., 1993). Cpn is an 85 kDa protein with an unusual, highly hydrophobic amino acid composition of $> 50\%$ proline, alanine, and valine residues; $\sim 10\%$ acidic residues; and very few basic residues. Moreover, it is also glutamic acid-rich with a strong negative charge (calculated pI, ~ 3.6). Cpn shows 26.7% identity with the crustacean DD4 protein, which may be involved in exoskeleton calcification (Endo et al., 2000).

Received May 22, 2012; revised Aug. 16, 2012; accepted Aug. 18, 2012.

Author contributions: S.W., B.K., and B.M. designed research; S.W., E.K., and D.D. performed research; M.L. and N.J.C. contributed unpublished reagents/analytic tools; S.W., B.K., M.P., M.K., and B.M. analyzed data; S.W. and B.M. wrote the paper.

This work was supported by grants from the U.S.–Israel Binational Science Foundation (B.M. and N.J.C.), the National Eye Institute (R01 EY03529 to B.M.), the Israel Science Foundation (B.M.), and the German Israeli Foundation (B.M.). We thank Dr. Varda-Shoshan-Barmatz for invaluable help in biochemical methodologies, and Drs. Roger Hardie, Franck Pichaud, Armin Huber, and Jeaseung Yoon for contributing a variety of transgenic flies used in this study. We also thank Drs. François Payre, Craig Montell, and the late Seymour Benzer for the antibodies against dMoesin, CalX, and Cpn, respectively; and Drs. Johannes Oberwinkler, David Zeevi, Shahar Frechter, and Moshe Parnas for very useful comments and critical reading of the manuscript. We also thank Ms. Naomi Feinstein for invaluable help in the EM studies.

The authors declare no competing financial interests.

Correspondence should be addressed to Baruch Minke, Department of Medical Neurobiology, Faculty of Medicine, The Hebrew University, Jerusalem 91120, Israel. E-mail: baruchm@ekmd.huji.ac.il.

DOI:10.1523/JNEUROSCI.2456-12.2012

Copyright © 2012 the authors 0270-6474/12/3014696-13\$15.00/0

Cpn has several unique properties that make it potentially important for cellular Ca^{2+} homeostasis: it was shown to bind Ca^{2+} *in vitro* and to reside in a region close to the rhabdomere. Visualization of Ca^{2+} in the rhabdomere region revealed Ca^{2+} precipitates in the same region where Cpn resides (Martin et al., 1993). Cpn mutants show a light-independent rough eye phenotype characterized by disorientation of the rhabdomeres and photoreceptor degeneration. This phenotype takes place in an early developmental stage, suggesting a role for Cpn in eye development (Ballinger et al., 1993). Until now, the function of Cpn in the adult fly has remained unknown.

Using transgenic *Drosophila* strains, we show that moderately reduced Cpn expression impaired Ca^{2+} homeostasis while Cpn elimination resulted in severe light-dependent photoreceptor degeneration. This degeneration was rescued by overexpression of the $\text{Na}^+ - \text{Ca}^{2+}$ exchanger. Ca^{2+} imaging showed that reduced Cpn levels resulted in abnormally fast kinetics of Ca^{2+} elevation in photoreceptors, indicating that Cpn constitutes an immobile Ca^{2+} buffer. Thus, the formation of a Ca^{2+} compartment by Cpn constitutes an effective new strategy to protect cells from Ca^{2+} overload and degeneration.

Materials and Methods

Fly stocks

Flies were raised at 24°C in a 12 h dark/light cycle. For each experiment, flies of either sex were treated and prepared as described below. For the electron micrograph (EM) experiments, flies were raised either in darkness to prevent light-induced retinal deformations or under intense illumination. For whole-cell recording experiments, flies were raised in 24 h darkness. The *CantonS* and *Rh1:Gal4* fly stocks were obtained from the Bloomington Stock Center. White-eyed *GMR:Gal4* flies were a gift from A. Huber. Red-eyed *GMR:Gal4* flies were obtained from J. Yoon. *CalX* overexpression strain was obtained from R. Hardie. Cpn transgenic strains were generated as described below. For determining light-dependent retinal degeneration, flies were kept in the dark or were illuminated with white light (Schott NG3 heat filter, cold light source KL1500, Schott) for 3–14 d. Dark-raised flies were dissected under dim red light (Schott RG 620, cold light source KL1500, Schott).

Generation and characterization of Cpn transgenes

Cpn RNAi transgenic strains were generated using the pWIZ vector as described previously (Lee and Carthew, 2003). Briefly, a construct encoding Cpn-inverted repeats was generated by amplifying a short segment of the Cpn coding sequence (GenBank Accession Number NM_169455) by PCR. This sequence was specifically designed to minimize predicted off-target effects. Two DNA fragments were subcloned, in opposite orientations, into the pWIZ plasmid to produce perfect RNA hairpin following splicing, under the yeast *UAS/Gal4* promoter. *UAS-Cpn-RNAi* flies were crossed with three different *GAL4* strains to drive differential Cpn expression. The *Gal4* driver lines that we used were driven by two different promoters: (1) the glass multimer reporter promoter (*P[GMR:Gal4]*), which is a strong promoter and drives expression in the whole-eye imaginal discs, and (2) the *Rh1* promoter (*P[Rh1:Gal4]*), the major rhodopsin promoter, which drives expression only in R1–R6 photoreceptor cells. A single *P[GMR:Gal4]* and three *P[Rh1:Gal4]* strains were used throughout this study. The *p[Rh1-Gal4]* strains that were used, *p[Rh1-Gal4](3)* and *p[Rh1-Gal4](X)*, derived a reduction in Cpn-expression level by 10% (*Cpn*^{90%}) or 50% (*Cpn*^{50%}), respectively. The *p[GMR-Gal4]* strain that was used derived reduction in Cpn-expression level by 99% (*Cpn*^{1%}). Because the *Cpn*^{1%} flies have <1% protein expression upon eclosion, we assumed that the effect of the RNAi could not become stronger as the flies aged. The *Cpn*^{50%} and *Cpn*^{90%} flies did not undergo age-dependent retinal degeneration [as tested by EM and deep pseudopupil (DPP); see Results], indicating that there was no change in the RNAi strength with age. This was also verified by Western blot analysis (data not shown). Transgenic flies expressing eGFP-tagged Cpn were generated by subcloning of eGFP and Cpn cDNA

into the pCasper-Rh1 vector. Both constructs were transformed into *Drosophila* and insertion strains containing a single copy of each transgene were generated by standard methods.

Western blots

Flies were collected 1 d posteclosion. To detect Cpn on Western blots, 30 fly heads were homogenized in a buffer solution (150 mM NaCl, 3 mM MgCl_2 , 10% glycerol, protease inhibitor, 50 mM HEPES, pH 7.4) and fractionated by centrifugation. Then the supernatant fraction was separated by 6% SDS-PAGE. Proteins were transferred for 2 h at 70–80 mA to BioTrace PVDF membranes (Pall) in Tris-glycine buffer. The blots were probed with mouse anti-Cpn primary antibodies (1:25 dilution, a kind gift from S. Benzer) or control antibodies and subsequently with goat anti-mouse IgG peroxidase conjugate. Signals were detected using ECL reagents (Biological Industries). Relative protein amounts were quantified using TINA2.0 software. The densities in each lane were normalized using the α Moesin (α -dMoe) signal (Chorna-Ornan et al., 2005) and calculated as a percentage of WT flies.

Electroretinogram and light stimulation

Electroretinogram (ERG) recordings were applied to intact flies as described previously (Peretz et al., 1994a). Orange light (OG 590 Schott edge filter) from a xenon high-pressure lamp (50 W, LPS 220, Photon Technology International) was delivered to the compound eye via a light guide. The maximal luminous intensity at the eye surface was ~ 2.5 logarithmic intensity units above the intensity for a half-maximal response of the major photoreceptors (R1–R6).

EM

For all EM experiments, Cpn-RNAi and *CantonS* (WT) flies were used. For the deformation/degeneration experiment, flies were divided into two groups before eclosion. One of them was raised at complete darkness while the other was raised at intense illumination conditions during the same period. Fly heads were separated and bisected longitudinally from flies at different ages: newly eclosed, 3, 7, or 14 d old. Tissues including compound eyes were dissected out of the flies in fixative solution (5% glutaraldehyde, 0.1 M cacodylate buffer, pH 7.4) and incubated overnight. Samples were then postfixed (1% OsO_4 , 0.1 M cacodylate buffer, pH 7.4), dehydrated through a graded series of ethanol, and embedded in epoxy resin. Ultrathin sections were stained with uranyl acetate and lead citrate, were observed with a Tecnai-12 transmission electron microscope (FEI) and photographed with a Mega-view II charge-coupled device camera (Philips).

Pigment granule migration

For the pigment granule migration experiment, 3-d-old dark-adapted flies were either dissected under dim red light (for <1 min, Schott RG 620 nm filter; longer illumination periods induced pigment granule migration in WT flies) and then incubated in Ringer's solution with or without 1 mM EGTA for 5 min in the dark before fixation (dark flies), or illuminated for 2 min and dissected in bright light before fixation (light flies). We could not analyze the *Cpn*^{1%} flies because pigment granules were not observed in the *Cpn*^{1%} flies and control flies (*P[GMR:Gal4]/+*). Pigment granule distance (μm) distribution from the base of the rhabdomere (for each strain/treatment $n \geq 250$ granules, $N = 2$ flies, see below) were analyzed. Using Kolmogorov–Smirnov test ($p < 0.001$), 100 random samples from each dataset (250–700 data points) were compared.

EM data analysis

For the deformation phenotype analysis in the different fly strains (see Figs. 2A*d*, 6E) fragmented, spliced, or missing rhabdomeres were counted as deformed rhabdomeres. Rhabdomere section areas (see Fig. 6F) and granule distances from the base of the rhabdomere (see Fig. 4B) were measured manually using the Tecnai-12 transmission electron microscope software (see Analysis).

Confocal microscopy

Dissected live retinas of Cpn-GFP;Act-RFP flies were visualized using the Fluoview confocal microscope (model 300 IX70; Olympus) with a Olympus UplanF1 60 \times /0.9 water objective. Optical sections were recorded

from the middle of the cell. RFP and GFP fluorescence were recorded sequentially using laser excitation wavelengths of 568 and 488 nm, respectively. Pictures are merged sequential images obtained by 568 nm, followed by 488 nm excitation lights, on separate channels.

Whole-cell recordings

Dissociated ommatidia were prepared from newly eclosed flies (<1 h posteclosion). Voltage-clamp whole-cell recordings were performed. Membrane potential was clamped to -70 mV and whole-cell capacitance was routinely measured. Signals were amplified using an Axopatch-200B (Molecular Devices) patch-clamp amplifier. Currents were sampled at 5 kHz using an analog-to-digital converter (Digidata 1200, Molecular Devices), filtered <1 kHz, and analyzed by the pClamp 9.2 software (Molecular Devices). Dark bumps were recorded ~ 1 min after whole-cell formation for ~ 2 min and analyzed off-line using the “threshold detection” application in the Clampfit 9.2 software (Molecular Devices). The following parameters were used: trigger, -3 pA; rearm, -2 pA; pretrigger, 1 ms; post-trigger, 1 ms; minimum allowed duration, 10 ms. Data were collected within 5 min of establishing the whole-cell configuration. The extracellular solution contained (in mM): 125 NaCl, 5 KCl, 10 TES (N-Tris-(hydroxymethyl)-methyl-2-amino-ethanesulphonic acid), 25 proline, 5 alanine. The whole-cell recording pipette solution contained (in mM): 140 K-gluconate, 2 $MgSO_4$, 10 TES, pH 7.15, 4 MgATP, 0.4 NaGTP, 1 NAD. $CaCl_2$ was added to the intracellular solution as indicated. Two-factor ANOVA with replication was performed to test whether the $[Ca^{2+}]_i$ in the recording pipette and the Cpn level affects bump frequency. One-factor ANOVA was used to test the Cpn protein level effect on bump frequency.

DPP monitoring

Newly eclosed WT, Cpn-RNAi, and CalX rescue flies were moved to a fresh vial and monitored for the presence of DPP every 2 d until the age of 11 d posteclosion. The percentages of flies retaining DPP on each day were plotted against their age (see Fig. 6B) (for each genotypic group, $n \geq 50$ flies).

Cell culture and transfections

HEK293 cells were grown as previously described under standard conditions (Parnas et al., 2009). Briefly, cells were grown in DMEM medium containing 10% FCS, penicillin, and streptomycin. For Cpn-GFP experiments, cells were transfected with pcDNA4-Cpn-GFP vector. For the Ca^{2+} -imaging experiments, cells were cotransfected with pcDNA4-Cpn, pcDNA3-TRPV1, pcDNA4-mCherry, and empty pcDNA4 vector. Transient expression of Cpn, TRPV1, mCherry, and Cpn-GFP was performed using TransIT-LT1 (Mirus Bio) and cells were analyzed ~ 24 h after transfections.

Ca^{2+} imaging

Photoreceptor cells. The excitation light of the calcium indicator also activated the photoreceptor cell. The cell-impermeable low-affinity fluorescent Ca^{2+} indicator calcium green 5N (Invitrogen) was delivered to the cell by the patch pipette. Whole-cell patch-clamp recordings were performed as described in whole-cell recordings above except that 0.4 mM Ca^{2+} and 4 mM Mg^{2+} were added to the extracellular solution and 100 μM calcium green 5N was added to the recording pipette. To reduce the buffering effect of the electrogenic Na^+-Ca^{2+} exchanger (CalX) and test the buffering effect of Cpn in isolation, we set the membrane voltage to 0 mV, a voltage that reduces the activity of the CalX by $\sim 70\%$ (Hardie, 1995). Simultaneous Ca^{2+} imaging and whole-cell recordings were performed. The whole-cell recordings were used to ensure that the photoreceptor cells were undamaged and respond to light normally. Light emitted from a xenon high-pressure lamp (Lambda LS, Sutter Instrument) was delivered to the ommatidia by epi-illumination via the objective lens. Images of cells were taken by a CCD camera (IX70, Andor Technology) at 45 Hz. Data were analyzed using ImageJ software (Abramoff et al., 2004). To estimate the relative change in $[Ca^{2+}]_i$, cellular fluorescence was sampled from the distal part of the photoreceptor cell, including both the rhabdomere and cell body. The cell fluorescence was normalized to pipette fluorescence ($\Delta F/F$) after background fluorescence was subtracted from both the cell and the pipette fluorescence. Time to peak was measured at 95% of maximum fluorescence.

HEK293 cells. Cytosolic calcium concentration was measured using the Fura-2 fluorescent indicator as described previously. Briefly, cells seeded on glass slides were incubated with 2 μM Fura-2 AM (Invitrogen) for 30 min in dark at 37°C. Following incubation, cells were washed with DMEM medium for 30 min. Cells were incubated in an extracellular solution (140 mM NaCl, 2.8 mM KCl, 1.2 mM $MgCl_2$, 10 mM D-glucose, 10 mM HEPES, 2 mM $CaCl_2$, pH 7.2, with NaOH) and then imaged using a CCD camera (IX70, Andor Technology). Cells loaded with Fura-2 were excited alternately with 340 and 380 nm illumination and the fluorescence emission images ratioed as an index of intracellular calcium. To demonstrate Ca^{2+} buffering by Cpn, Cpn was coexpressed together with the Ca^{2+} -permeable TRPV1 channel, which can be robustly activated by application of capsaicin (1 μM in the above extracellular solution). For each experiment, 10–30 cells were simultaneously monitored and their fluorescence emission ratios averaged at the end of recording. Fluorescence 340:380 ratio was normalized to basal ratio before the application of capsaicin $[R(340:380)/R_0(340:380)]$. Cells were imaged by a CCD camera (IX70, Andor Technology) at 45 Hz. Data were analyzed using ImageJ software (Abramoff et al., 2004).

Results

Generation of transgenic strains in which Cpn-expression levels are reduced in a graded manner

In a previous study, Cpn mutants exhibited rough eyes and morphological deformations during development, suggesting a developmental role for Cpn (Yang and Ballinger, 1994). To search for other possible Cpn functions, we generated transgenic *Drosophila* strains in which Cpn-expression levels were reduced in a graded manner in adult flies. In addition, GFP-tagged Cpn was expressed to accurately localize Cpn in living photoreceptor cells. Confocal microscope images of isolated retinæ from transgenic flies expressing GFP-tagged Cpn (Rh1:Cpn-GFP), confirmed the earlier observation of Benzer, Miller, and colleagues (Martin et al., 1993) that Cpn is exclusively localized to the cytoplasmic region adjacent to the rhabdomere. Longitudinal (Fig. 1Aa) and cross (Fig. 1Ab) optical sections revealed that the fluorescent image of the Cpn-GFP fusion protein was localized at the cytoplasmic area adjacent to the microvilli, consistent with the previous localization of Cpn obtained by immune EM cross sections.

Cpn mutant strains, generated by Yang and Ballinger (1994), revealed severe retinal deformations at early development and no light-dependent phenotypes, which precluded functional analyses. We, therefore, investigated the role of Cpn in adult flies using an RNAi-based approach, which allowed more refined and functional analyses. To establish flies in which Cpn expression is reduced in a graded manner, we have generated a P[UAS:Cpn-RNAi] strain. P[UAS:Cpn-RNAi] flies were crossed with different Gal4 driver lines (see Materials and Methods). Progeny of these crosses revealed, by Western blot analysis, Cpn-expression level of 1%, 50%, and 90% (Fig. 1B, C) relative to WT flies, and were used in further studies. In this work, we refer to the progeny of these crosses as Cpn^{1%}, Cpn^{50%}, and Cpn^{90%}. The expression levels of the major phototransduction proteins (e.g., rhodopsin, Gq α , phospholipase C, TRP, TRP-like, CalX, dMoesin, and calnexin) in Cpn-RNAi flies were found to be similar to those of WT flies (data not shown).

Severe reduction of Cpn expression causes light-dependent defects in photoreceptor morphology

Having established *Drosophila* flies with graded reduction of Cpn expression, we proceeded to investigate the effects of this reduction on adult photoreceptor cell morphology. EMs of thin retinal sections taken from dark-raised and light-raised flies of different Cpn-RNAi progeny revealed normal retinal morphology in flies in which Cpn expression was moderately reduced (Cpn^{90%}, Fig.

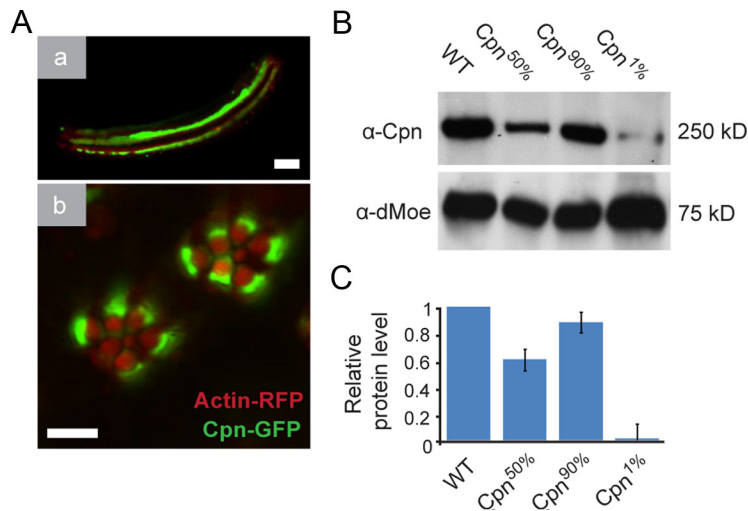


Figure 1. Generation and characterization of transgenic strains in which Cpn expression level is reduced in a graded manner. **A**, Longitudinal (**a**) and cross (**b**) confocal microscopic optical sections showing the localization of GFP-tagged Cpn (green) with relation to the rhabdomeres (marked by RFP-tagged actin, red). Scale bars, 5 μ m. **B**, Western blot analysis showing Cpn protein level in Cpn-RNAi flies. **C**, Histogram presenting the quantification of the data (mean \pm SEM, $n = 4$).

2Ac). When Cpn expression was nearly eliminated (Cpn^{1%}), transgenic flies reared in the dark displayed only mild retinal deformations at a young age of 3 d after eclosion (Fig. 2Ad). However, the deformation phenotypes further deteriorated when Cpn^{1%} flies were raised under continuous illumination for 3 d (Fig. 2Ae). A large fraction of photoreceptor cells had deformed rhabdomeres (Fig. 2Ae, see Fig. 6G for quantification, see also Materials and Methods) and rhabdomere cross-section areas were smaller compared with those of WT flies (Figs. 2Aa, see Fig. 6E,F for quantification) or of P[GMR:Gal4]/+ control flies (Fig. 2Ab). Since P[GMR:Gal4]/+ control flies showed no significant morphological differences compared with WT flies, we used WT as a control in the following experiments. The reduction in rhabdomere size of Cpn^{1%} flies is also manifested in whole-cell recordings of photoreceptor capacitance, which directly reflects the surface membrane area. Overall, the whole-cell capacitance in transgenic Cpn^{1%} flies relative to control flies (WT and P[GMR:Gal4]/+) was reduced from ~55 to ~40 pF (Fig. 2B, $p < 0.05$). These results indicate that, in addition to photoreceptor development, Cpn is also required for the maintenance of photoreceptor cells in adult flies (see below).

Elimination of Cpn expression abolishes the physical separation between the rhabdomere and cell body

In WT flies, the cytoplasm adjacent to the rhabdomere base, where Cpn resides, is referred to as the rhabdomere terminal web (RTW) (Chang and Ready, 2000). The RTW, which extends from the rhabdomere base deep into the photoreceptor cytoplasm, is characterized by a virtually organelle-free region. Thus, in a typical EM thin section of *Drosophila* retina, the RTW region appears electron transparent (Fig. 2Aa, Ba). Endoplasmic reticulum (ER) and mitochondria are distributed along the entire length of the photoreceptor cell body and reside in close proximity, but outside the RTW (Chang and Ready, 2000). In a marked difference to the morphology of WT photoreceptor cells, the electron transparent appearance of the RTW and low organelle density were missing in Cpn^{1%} flies. In these transgenic flies, the subrhabdomeral area was filled with cellular organelles, such as ERs and mitochondria (Fig. 2Cc, identified by their common morphological characteristics, Fig. 2Cb, and a magnification). In contrast, the RTW transparent appearance was normal in Cpn^{90%} photo-

receptor cells (Fig. 2Ab), indicating that a small reduction in Cpn-expression level does not lead to cellular morphology deformations. Thus, the absence of the RTW in Cpn^{1%} photoreceptor cells indicates that Cpn has an essential role in physical separation of the rhabdomere from the cell body.

Elimination of Cpn induces severe light-dependent photoreceptor degeneration

Exposure of Cpn^{1%} flies to illumination for 3 d resulted in deformations of rhabdomere morphology and significant reduction of rhabdomeric size (Fig. 2, see Fig. 6). Further exposure of Cpn^{1%} flies to continuous illumination for 7 d induced severe photoreceptor degeneration, while no significant degeneration was observed in either WT flies raised under continuous illumination for 7 d or in dark-raised Cpn^{1%} flies (Fig. 3). Furthermore, most rhabdomeres of 7-d-illuminated Cpn^{1%} flies were either missing or strongly deformed, and the cell body appeared inundated with rough endoplasmic reticulum (rER) relative to WT photoreceptors (Fig. 3E). Similar accumulation of rER was observed in dark-raised Cpn^{1%} flies. Further exposure of the Cpn^{1%} flies to 14 d of continuous illumination virtually eliminated all R1–R6 photoreceptor cells while only a few of the UV-absorbing central photoreceptor cells (R7, R8) remained in degenerated form (Fig. 3F). In WT flies exposed to the same illumination conditions for 7 or 14 d, no significant degeneration was observed (Fig. 3A, D). Similarly, Cpn^{1%} flies raised in the dark for 7 d showed relatively mild retinal deformation (Fig. 3B) and Cpn^{1%} flies raised in the dark for 14 d still maintained all rhabdomeres, but with deformed morphology (Fig. 3C).

Together, these results show that Cpn is essential for maintaining the structural integrity of the photoreceptor cells during prolonged illumination, while its absence induces severe light-dependent photoreceptor degeneration.

Application of sensitive bioassays to detect abnormal Ca²⁺ homeostasis in Cpn hypomorph flies that preserve normal morphology

The strategic localization of Cpn, filling the entire cytoplasmic volume between the rhabdomere and the cell body and its Ca²⁺ binding property, led Martin and colleagues to propose that Cpn might function as a Ca²⁺-sequestering “sponge” that regulates the amount of cytosolic Ca²⁺. They furthermore speculated that it functions as a Ca²⁺ store. However, this hypothesis has never been examined. Furthermore, the Cpn-Ca²⁺ stoichiometry was determined as 0.3 (i.e., 1 mol of Cpn binds 0.3 mol of Ca²⁺), implicating negligible Ca²⁺-binding capacity (Martin et al., 1993).

The possible involvement of Cpn in Ca²⁺ homeostasis and the morphological changes associated with highly reduced Cpn-expression levels raises the question of causality: (1) impaired Ca²⁺ homeostasis may lead to photoreceptor degeneration or (2) cellular degeneration can lead to impaired Ca²⁺ homeostasis. To determine which of these two possibilities is true, we tested Ca²⁺ homeostasis in Cpn-RNAi flies, in which relatively small reduction in Cpn level (Cpn^{90%} and Cpn^{50%}) did not cause any sign of morphological changes (Fig. 2Ab). If Cpn indeed has a role in

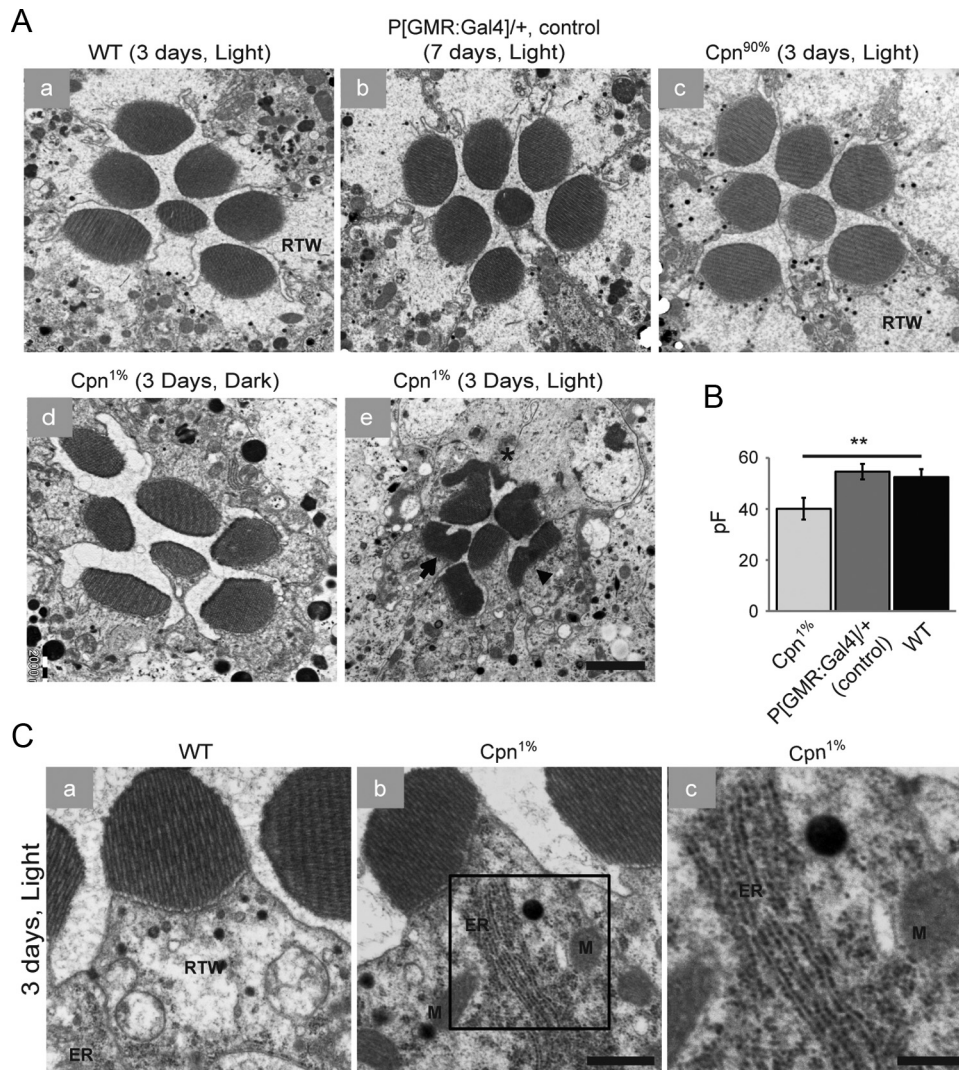


Figure 2. Transgenic flies in which Cpn is nearly eliminated undergo light-dependent photoreceptor morphological deformations a few days after eclosion. Thin EM sections of 3-d-old WT and Cpn-RNAi ommatidia. **A**, EM section of WT (**a**), P[GMR:Gal4]/+ control (**b**), Cpn^{90%} (**c**), Cpn^{1%} raised in complete darkness (**d**), and Cpn^{1%} raised under continuous illumination (**e**). When Cpn^{1%} flies were raised in constant illumination, many rhabdomeres are either spliced (**e**, arrow), show short microvilli (**e**, arrowhead), or are missing (**e**, asterisk). Scale bar, 2 μm . Note the absence of pigment granules in Cpn^{1%} flies. **B**, Whole-cell capacitance measurements from isolated ommatidia of WT and Cpn^{1%} photoreceptors. The capacitance measurements show significant reduction in cellular capacitance of the Cpn^{1%} relative to control and WT photoreceptors (mean \pm SEM, $**p < 0.05$, $n = 13$). **C**, Magnified single rhabdomeres showing the normal electron transparent appearance of the RTW adjacent to the microvilli of WT flies (**a**). In Cpn^{1%} photoreceptors (**b**), the subrhabdomeral area is filled with cellular organelles such as ER and mitochondria (M). Scale bar, 500 nm. **c**, Inset of the subrhabdomeral cytoplasm from Cpn^{1%} fly, showing the proximity of cellular organelles to the base of the rhabdomere. Scale bar, 250 nm.

cellular Ca^{2+} homeostasis, a small reduction in Cpn-expression level is expected to cause only small changes in Ca^{2+} homeostasis. Therefore, we estimated the *in vivo* cell body or rhabdomeral $[\text{Ca}^{2+}]$ by using two different highly sensitive bioassays capable of comparing Ca^{2+} levels between WT and transgenic flies.

Reduced Cpn expression affects pigment granule migration

During light, an assembly of pigment granules migrates from the cell body and accumulates close to the cytoplasmic face of the rhabdomere (Franceschini and Kirschfeld, 1976; Satoh et al., 2008). It has been well established that light-induced elevation of cytosolic $[\text{Ca}^{2+}]$ triggers the migration of the pigment granules in WT flies (Kirschfeld and Vogt, 1980). In contrast, the pigment granules fail to localize near the rhabdomere during prolonged light in a mutant deficient of Ca^{2+} -permeable TRP channels (Cosens and Perry, 1972; Lo and Pak, 1981). Thus, pigment granule localization was used as a sensitive biosensor reporting on impaired cytosolic Ca^{2+} homeostasis.

Because of the extreme sensitivity of pigment granule migration to light-induced Ca^{2+} elevation (Satoh et al., 2008), dim red light was used during dissection to prevent pigment granule movement in dark-adapted WT flies (see Materials and Methods). We confirmed previous findings and showed that in dark-adapted WT flies the pigment granules were located at a distance from the rhabdomere (Fig. 4Aa, Aa', Fig. 4Ac, histogram; for details, see Materials and Methods). Upon illumination, the pigment granules moved through the Cpn region toward the base of the rhabdomere (Fig. 4Ab, Ab', Ac) (Satoh et al., 2008). Strikingly, in contrast to WT flies, even a small (10%) reduction of Cpn expression was sufficient to impair the normal pigment granule migration. Accordingly, in dark-adapted Cpn^{90%} flies, under the same experimental conditions, the pigment granules were localized close to the rhabdomere (Fig. 4B). This pigment granule localization is typical for light-adapted position in WT flies (Fig. 4Ab, Ab').

Localization of the pigment granules to the light-adapted state in dark-raised Cpn^{90%} flies suggests that Ca^{2+} levels are abnor-

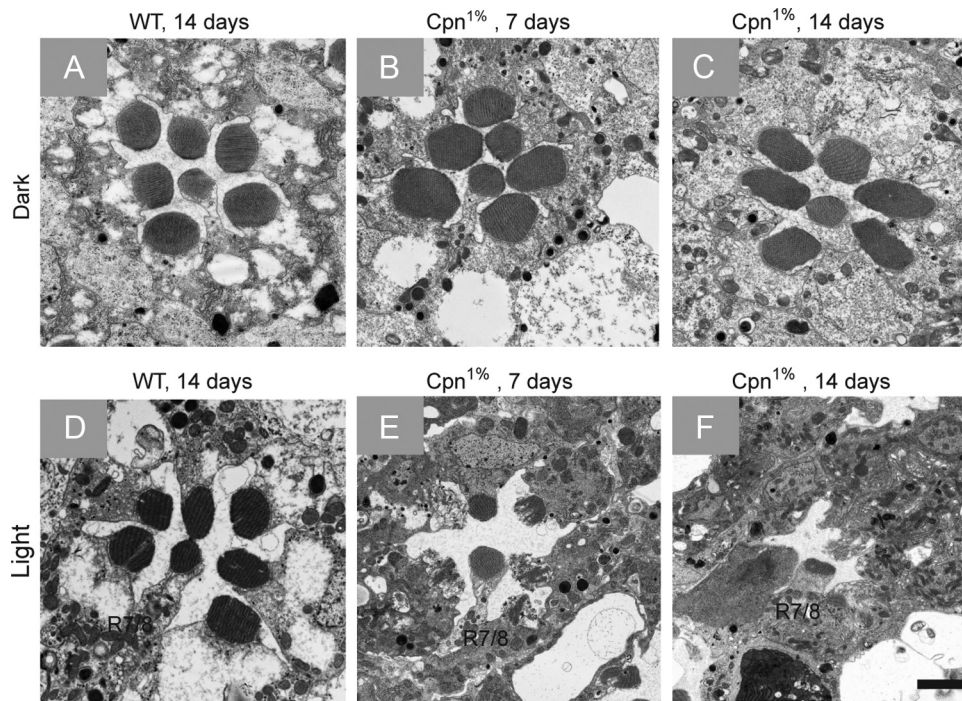


Figure 3. Age and light-dependent degeneration of $\text{Cpn}^{1\%}$ photoreceptors. *A–C*, Thin EM sections of WT (*A*) and $\text{Cpn}^{1\%}$ flies raised in darkness for 7 d (*B*) or 14 d (*C*) showing minor age-dependent retinal deformations. *D–F*, $\text{Cpn}^{1\%}$ flies reared for 7 d (*E*) or 14 d (*F*) under constant illumination undergo severe age-dependent and light-dependent retinal degeneration compared with WT flies (*D*). Scale bar, 2 μm .

mally elevated in the cell body under the experimental conditions used (see Materials and Methods and Discussion). To show the Ca^{2+} dependence of the pigment granule localization, we reduced the photoreceptor $[\text{Ca}^{2+}]$ by incubating the $\text{Cpn}^{50\%}$ fly eyes in Ringer's solution, without added Ca^{2+} but with 1 mM EGTA, before fixation for EM sections (see Materials and Methods). Figure 4*Ca,Ca'* shows that under these conditions the pigment granules of $\text{Cpn}^{50\%}$ flies were observed at a distance from the rhabdomere similar to their localization in dark-adapted WT flies. The migration of the pigment granules back to the dark position demonstrates that $[\text{Ca}^{2+}]$ is the sole determinant of the abnormal pigment granule localization in $\text{Cpn}^{90\%}$ flies. The distribution of the distances of the pigment granules from the base of the rhabdomeres is presented in Figure 4*Ac* (WT), 4*Bc* ($\text{Cpn}^{90\%}$), and 4*Cb* ($\text{Cpn}^{50\%}$, treated with EGTA). Pigment granules of dark-adapted WT flies and $\text{Cpn}^{50\%}$ flies treated with EGTA were localized at a similar distance from the rhabdomere base. Moreover, pigment granules of light-adapted WT and both light-adapted and dark-adapted Cpn -RNAi flies were localized in a similar light-adapted position, suggesting impaired Ca^{2+} homeostasis in transgenic flies.

Reduced Cpn expression affects the rate of dark bumps

We next applied a novel and sensitive bioassay, which critically depends on rhabdomeral Ca^{2+} levels following artificial Ca^{2+} elevation in the cell body, using whole-cell patch-clamp recordings (Katz and Minke, 2012). In WT flies, spontaneous unitary events (dark bumps), similar to single photon responses but smaller in amplitude, are observed in normal Ringer's solution. These dark bumps are Ca^{2+} -dependent and are the consequence of spontaneous GDP–GTP exchange on the $\text{Gq}\alpha$ subunit (Elia et al., 2005). A recent study has shown that, when Ca^{2+} was omitted from the extracellular solution, dark bumps were virtually absent ($<2 \text{ min}^{-1}$), while, in the presence of Ca^{2+} , dark bumps were

readily observed. Furthermore, it was shown that, in the absence of extracellular Ca^{2+} , when $[\text{Ca}^{2+}]$ was highly increased in the cell body, dark bumps reappeared (Katz and Minke, 2012) (see Fig. 5). Since the entire bump production machinery exclusively resides in the rhabdomere, this assay reflects Ca^{2+} levels in the rhabdomere.

To compare the effect of artificially increasing cell body $[\text{Ca}^{2+}]$ on rhabdomeric Ca^{2+} levels between WT and $\text{Cpn}^{90\%}$ flies, we used the Ca^{2+} dependence of dark-bump formation. We found that an increase of $[\text{Ca}^{2+}]$ in the cell body increased the rate of dark bumps, which are produced in the rhabdomere (Fig. 5*A*) (Katz and Minke, 2012) (see Materials and Methods). At nominal (i.e., few μM) extracellular Ca^{2+} , when using intracellular solution with no added Ca^{2+} , no dark bumps were observed in either WT or $\text{Cpn}^{90\%}$ flies (Fig. 5*A*). When 1.5 mM Ca^{2+} was included in the intracellular solution, only sporadic dark bumps were observed in WT flies while a considerably higher rate of dark bumps was observed in $\text{Cpn}^{90\%}$ flies (Fig. 5*A*, middle; Fig. 5*B*). Further elevation of intracellular $[\text{Ca}^{2+}]$ to 3 mM resulted in the appearance of dark bumps in WT and a significantly higher bump rate in $\text{Cpn}^{90\%}$ flies (Fig. 5*A*, bottom; Fig. 5*B*). The experiments performed on WT flies showed that cell-body Ca^{2+} had limited access to the rhabdomere and this limited access can be overcome by including very high $[\text{Ca}^{2+}]$ in the pipette. Reduced Cpn expression in $\text{Cpn}^{90\%}$ flies can also overcome the limited access of Ca^{2+} to the rhabdomere. The results of Figure 5*A* suggest that at a given cell body $[\text{Ca}^{2+}]$ an increased bump rate should be observed when Cpn expression is further reduced. Consistent with this prediction, the frequency of the dark bumps was significantly higher in $\text{Cpn}^{50\%}$ flies than in $\text{Cpn}^{90\%}$ flies when 3 mM $[\text{Ca}^{2+}]$ was included in the recording pipette (Fig. 5*C,D*).

Altered cellular morphology can affect cellular diffusion of Ca^{2+} , leading to impaired Ca^{2+} homeostasis. The EM sections of

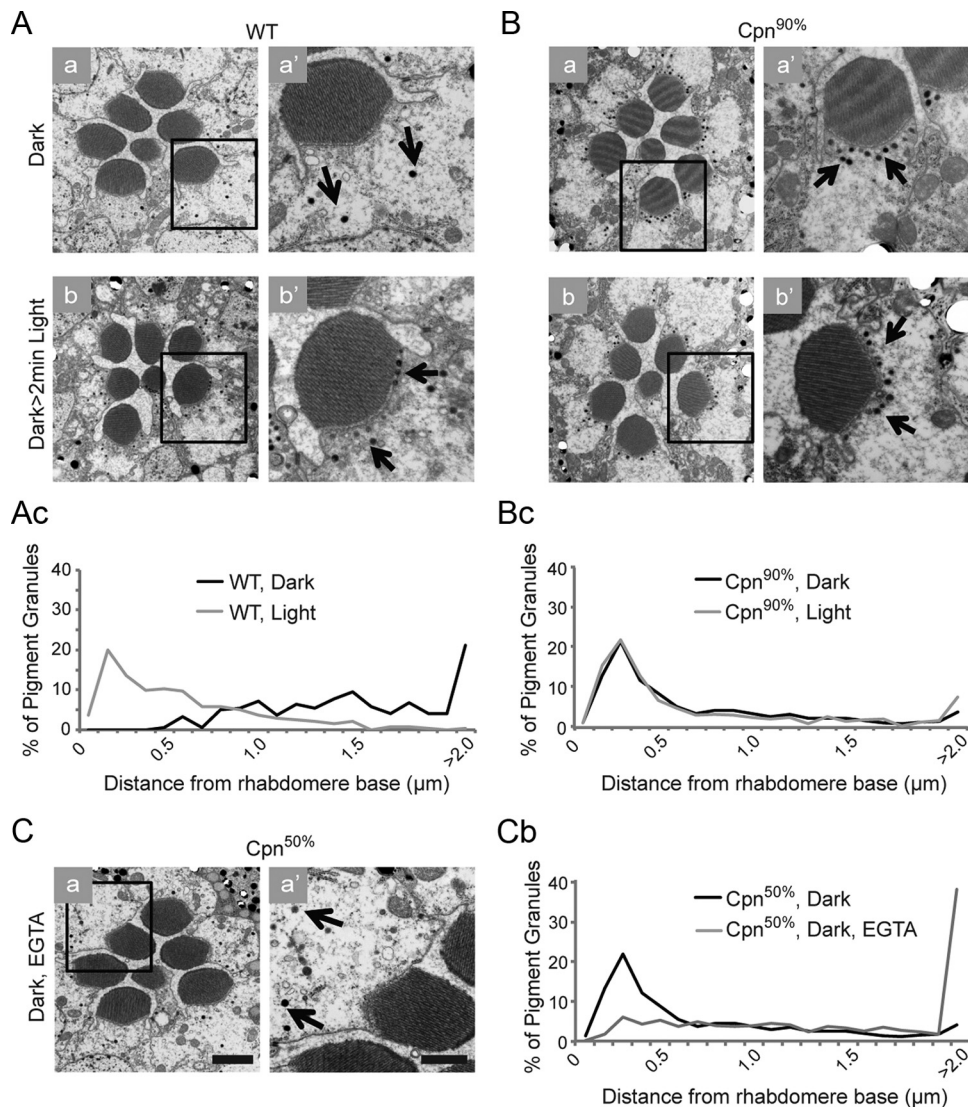


Figure 4. Reduced Cpn level affects migration of pigment granules. **A, B**, EM thin sections of retinæ from dark-adapted (**Aa, Aa'**) or illuminated (2 min, **Ab, Ab'**) WT flies, and dark-adapted (**Ba, Ba'**) or illuminated (**Bb, Bb'**) Cpn^{90%} flies. In Cpn^{90%} flies, the pigment granules (inset, arrows) are localized permanently close to the rhabdomere in a typical light-adapted position, regardless of dark/light regime. The EM picture of single rhabdomeres (inset) is magnified on the right. **C**, When incubating Cpn^{50%} flies, in Ca^{2+} -free solution (1 mM EGTA) before fixation, the pigment granules of Cpn^{50%} flies (inset, arrows) are localized away from the rhabdomere in a typical dark-adapted position (**a, a'**). The scale bar of **Ca, 2 μm** refers also to **Aa, Ab, Ba, Bb**. The scale bar of **Ca', 1 μm** refers also to **Aa', Ab', Ba', Bb'**. **Ac, Bc, Cb**, Pigment granules distances (μm) distribution from the base of the rhabdomere (for each strain/treatment, $n \geq 250$ granules, $N = 2$ flies). From each dataset (250–700 data points), 100 random samples were compared by using Kolmogorov–Smirnov test ($p < 0.001$).

Figure 2 show no morphological abnormalities, while the sensitive Ca^{2+} -dependent bioassays of Figures 4 and 5 clearly show impaired Ca^{2+} homeostasis in hypomorph Cpn-RNAi flies. Therefore, the impaired Ca^{2+} homeostasis does not result from morphological changes but rather from direct Cpn involvement in Ca^{2+} homeostasis.

The effect of reduced Cpn expression on the physiological response to light

Since Ca^{2+} is known to have multiple effects on fly phototransduction (Hardie and Raghu, 2001; Katz and Minke, 2009), it was of interest to examine the electrical response to light in flies with reduced Cpn-expression levels.

Dark-adapted Cpn^{1%} flies were characterized using the ERG, which is the summed electrical activity of the entire eye recorded *in vivo* (Peretz et al., 1994b), as well as by whole-cell recordings from isolated ommatidia. At all light intensities, the Cpn^{1%} flies

displayed normal ERG waveform but significantly reduced amplitude of the ERG light response relative to WT flies (Fig. 6C,D, green and red). The reduction in ERG amplitude of Cpn^{1%} flies is consistent with an abnormally elevated $[\text{Ca}^{2+}]$ in the cells of Cpn^{1%} flies under the experimental conditions used (flies were mounted under dim red light; see Materials and Methods, Discussion). Elevated levels of cellular Ca^{2+} are known to reduce the amplitude of the macroscopic response to light because it induces light adaptation (Gu et al., 2005). The normal waveform of the ERG response to light (Fig. 6C,D) and of the light-induced current (data not shown) of the Cpn^{1%} flies suggests that Cpn has no role in shaping the light response and therefore plays no direct role in the phototransduction cascade. Nevertheless, its effect on cellular Ca^{2+} homeostasis has an indirect effect on the response amplitude. The electrophysiological data thus give additional independent evidence that Cpn is important for cellular Ca^{2+} homeostasis.

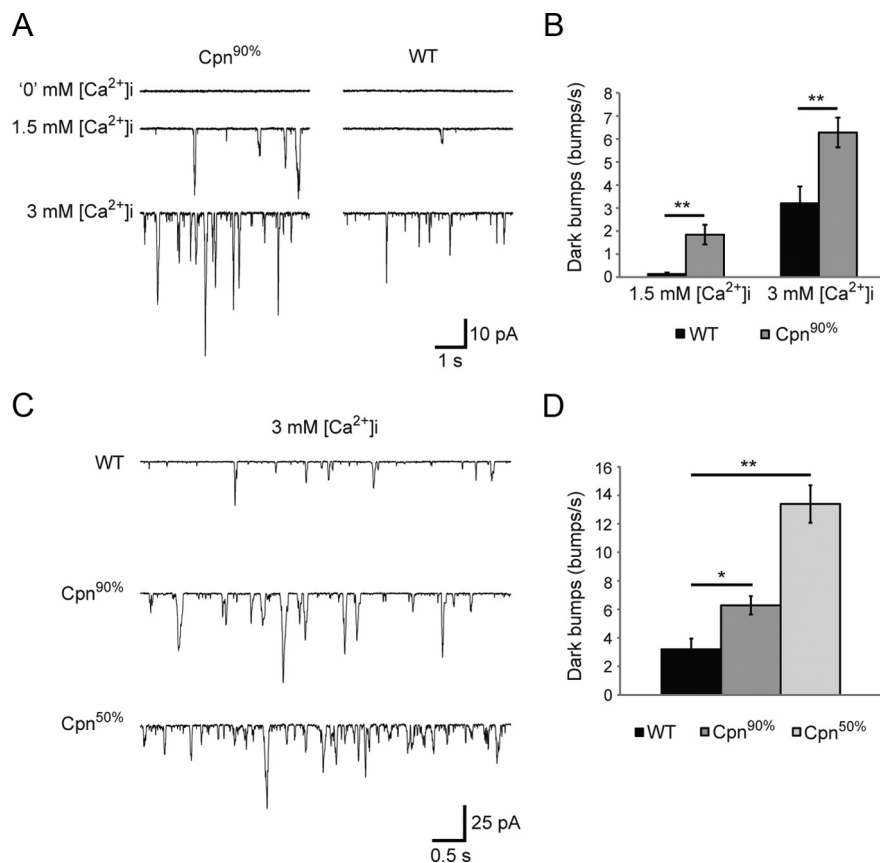


Figure 5. Reduced Cpn level affects the rate of single photon-like events in the dark. **A**, Whole-cell recordings from WT and Cpn^{90%}-transgenic flies in the dark at low-divalent external solution (upper traces), with added 1.5 mM (middle traces) or 3 mM [Ca²⁺]_i (bottom traces) in the recording pipette. Elevating intracellular [Ca²⁺]_i induced the appearance of dark bumps in WT flies, but much higher frequency was observed in Cpn^{90%}-transgenic flies. **B**, Histogram comparing bump frequency between WT and transgenic Cpn^{90%} flies when different [Ca²⁺]_i were included in the recording pipette. Only bumps with amplitudes larger than 3 pA were counted (mean ± SEM, *n* = 3, ***p* < 0.01). **C**, Whole-cell recordings from WT, Cpn^{90%}, and Cpn^{50%} flies in the dark at low-divalent external solution, when 3 mM [Ca²⁺]_i was included in the recording pipette. Note, the increase in dark-bump frequency as Cpn level is reduced. **D**, Histogram comparing bump frequency between WT, Cpn^{90%}, and Cpn^{50%} flies in 3 mM [Ca²⁺]_i (mean ± SEM, *n* = 3, **p* < 0.05, ***p* < 0.01). Result from single-factor ANOVA revealed a significant effect of Cpn level on the bump frequency (*p* < 0.001).

Rapid removal of calcium by overexpressing the Na⁺-Ca²⁺ exchanger CalX rescues most of the Cpn^{1%} phenotypes

The results presented above (Figs. 4, 5, 6C,D) suggest that the observed phenotypes are a consequence of abnormal Ca²⁺ homeostasis in the photoreceptor cells of Cpn-RNAi flies. The major regulator of rhabdomeral [Ca²⁺]_i is the Na⁺-Ca²⁺ exchanger, CalX. During illumination, in WT flies, Ca²⁺ influx leads to an elevated rhabdomeral [Ca²⁺]_i and its extrusion by CalX prevents Ca²⁺ overload in the photoreceptor cell body (Wang et al., 2005). However, in the absence of Cpn, an abnormally elevated level of Ca²⁺ in the cell body, where CalX is absent, may occur. Therefore, during prolonged illumination for several days, the normal expression level of CalX may not be sufficient to prevent Ca²⁺ overload in the cell body of Cpn^{1%} flies, leading to photoreceptor degeneration.

To test the validity of this scenario, we generated triple-transgenic flies overexpressing CalX (under the control of the Rh1 promoter, Rh1:CalX; Fig. 6A), on the background of Cpn^{1%} (Cpn^{1%}/Rh1:CalX). Previous studies showed that the CalX-null mutant reveals persistently high cytosolic Ca²⁺ levels following illumination, as implicated from the small amplitude of the light-induced bump. Furthermore, the CalX-overexpressing fly, showing large exchange current and massive Ca²⁺ extrusion, par-

tially rescues Ca²⁺ overload-induced degeneration (Wang et al., 2005).

We first analyzed the presence of the DPP (Franceschini and Kirschfeld, 1971b; Iakhine et al., 2004) (see Materials and Methods). The DPP is the superposition of virtual images of rhabdomeres in adjacent ommatidia observed when a low-power microscope is focused at the center of curvature of the compound eye of flies (Franceschini and Kirschfeld, 1971a). It constitutes an indirect, but very sensitive method to determine the integrity of the rhabdomeres (Iakhine et al., 2004). WT flies exhibit a DPP regardless of their age or growing conditions. In contrast, only ~30% of Cpn^{1%} flies displayed a DPP upon eclosion, and by 7 d posteclosion, when raised in a 12 h dark/light cycle regime, the DPP was eliminated in most flies. However, when raised in the dark, Cpn^{1%} flies showing a DPP upon eclosion did not lose the DPP, even at 11 d posteclosion. Strikingly, almost 90% of Cpn^{1%}/Rh1:CalX flies, regardless of age, exhibited a DPP (Fig. 6B). This result demonstrates a significant rescue of the degenerated rhabdomeric morphology in Cpn^{1%} flies by CalX overexpression.

To further support the rescue of the Cpn^{1%} phenotype by CalX overexpression in young flies, we examined photoreceptor morphology using EM. Cpn^{1%}/Rh1:CalX flies raised under various conditions (Fig. 2) exhibited relatively normal rhabdomere morphology of size and shape in most photoreceptor cells compared with Cpn^{1%} flies (Fig. 6E–G). However, because these flies still lack Cpn, the electron transparent appearance of the RTW was not observed in Cpn^{1%}/Rh1:CalX flies.

To assess the ability of CalX overexpression to rescue photoreceptor degeneration under prolonged illumination, photoreceptor degeneration was compared between Cpn^{1%} and the Cpn^{1%}/Rh1:CalX flies. In contrast to Cpn^{1%} flies, Cpn^{1%}/Rh1:CalX flies showed a significant morphological rescue, as judged by the reappearance of the rhabdomeres (Fig. 7A,B). We also examined possible rescue of the physiological phenotype arising from reduced Cpn levels. ERG responses to light were compared between Cpn^{1%} and the Cpn^{1%}/Rh1:CalX flies. As shown in Figure 6C, Cpn^{1%}/Rh1:CalX flies showed partial rescue of the ERG response amplitudes at moderate and intense light relative to Cpn^{1%} flies. This result demonstrates that the reduction of ERG amplitude in Cpn-deficient flies (Fig. 6C,D) is due to abnormally elevated [Ca²⁺]_i in the photoreceptor cell.

Altogether, the rescue of the structural and functional phenotypes of Cpn-deficient flies by CalX overexpression strongly supports the notion that the major role of Cpn is to establish the rhabdomere as a Ca²⁺-segregated compartment. This important function prevents Ca²⁺ overload in the cell body of fly photoreceptors during continuous illumination.

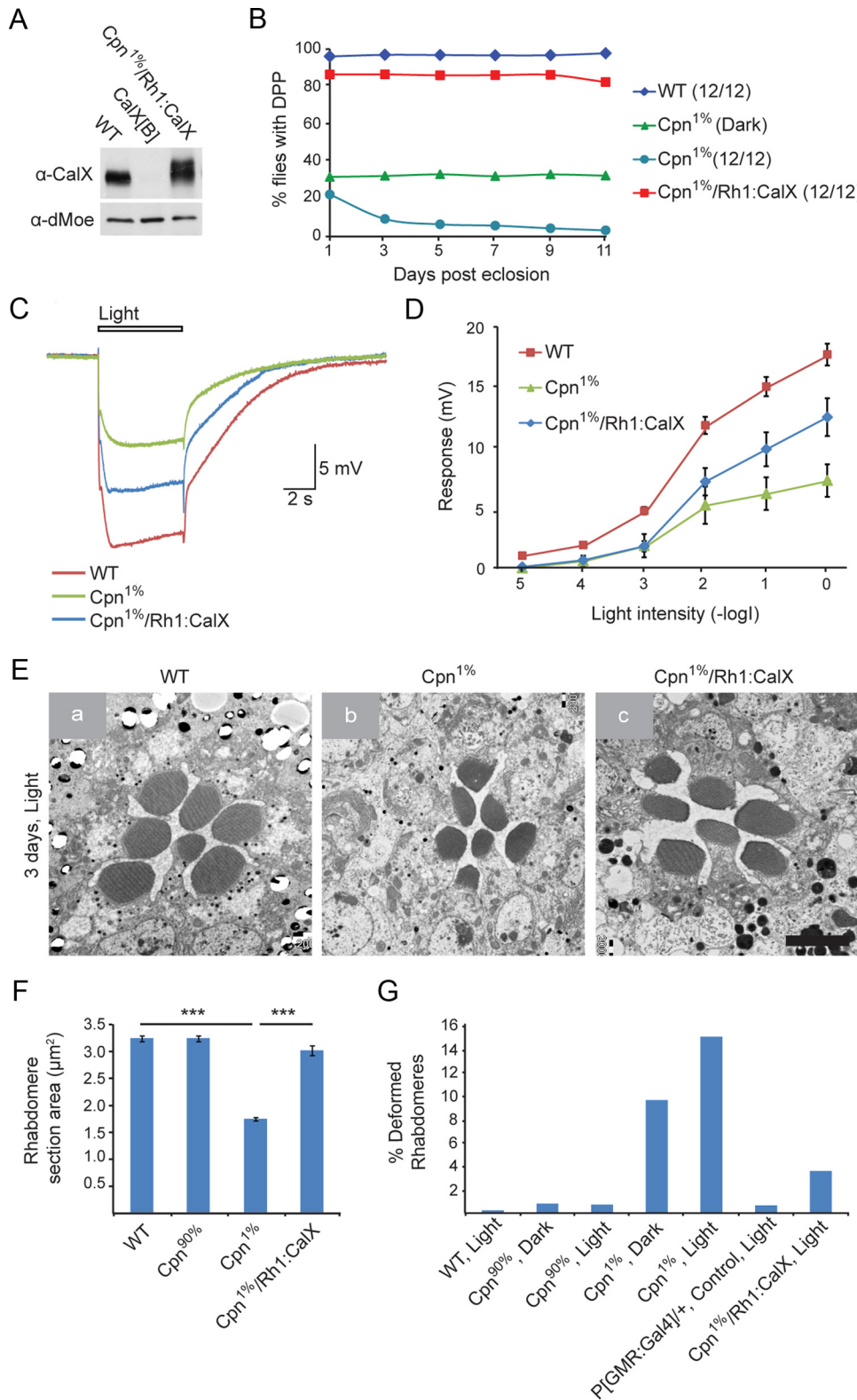


Figure 6. Rapid removal of Ca²⁺ by overexpressing CalX rescued most of the Cpn^{1%} phenotypes at young age. **A**, Western blot analysis of CalX protein level in WT, Cpn-RNAi lines, and CalX[B] (a null allele) showing normal expression of CalX in Cpn-RNAi flies. **B**, Graphs showing percentage of flies with DPP in the compound eyes of live intact flies. Flies were raised either in 12 h dark/light regime or in darkness. Overexpressing CalX rescued the lack of DPP in light-raised Cpn^{1%} ($n \geq 50$). **C, D**, Comparison of ERG responses to the maximal intensity orange light pulse among Cpn^{1%} and WT flies. **C**, Superimposition of three sample traces showing the ERG responses of WT, Cpn^{1%}, and Cpn^{1%}/Rh1:CalX rescue flies. **D**, Intensity–response curve of ERG responses. The different curves were measured from WT, Cpn^{1%}, and Cpn^{1%}/Rh1:CalX flies (mean \pm SEM, $n = 4–8$). **E**, EM thin sections of retinas from WT (**a**), Cpn^{1%} (**b**), and Cpn^{1%}/Rh1:CalX (**c**) flies. The EM cross sections reveal a significant reduction in rhabdomere area of Cpn^{1%} relative to WT. Overexpressing CalX rescues the original rhabdomere size. Scale bar, 2 μ m. **F**, Histogram plotting the mean rhabdomere cross-section area (μ m²) of WT, Cpn^{90%}, Cpn^{1%}, and Cpn^{1%}/Rh1:CalX photoreceptor cells (mean \pm SEM, $n > 100$ rhabdomeres, $N = 2$ flies, ANOVA $p < 0.01$). **G**, Quantification of the various rhabdomere deformation phenotypes in different flies as indicated. Overexpressing CalX rescues Cpn^{1%} deformation phenotypes. Deformed rhabdomeres included fragmented, spliced, flattened, or missing rhabdomeres (see Fig. 2; $n > 100$ photoreceptor cells, $N = 2$ flies).

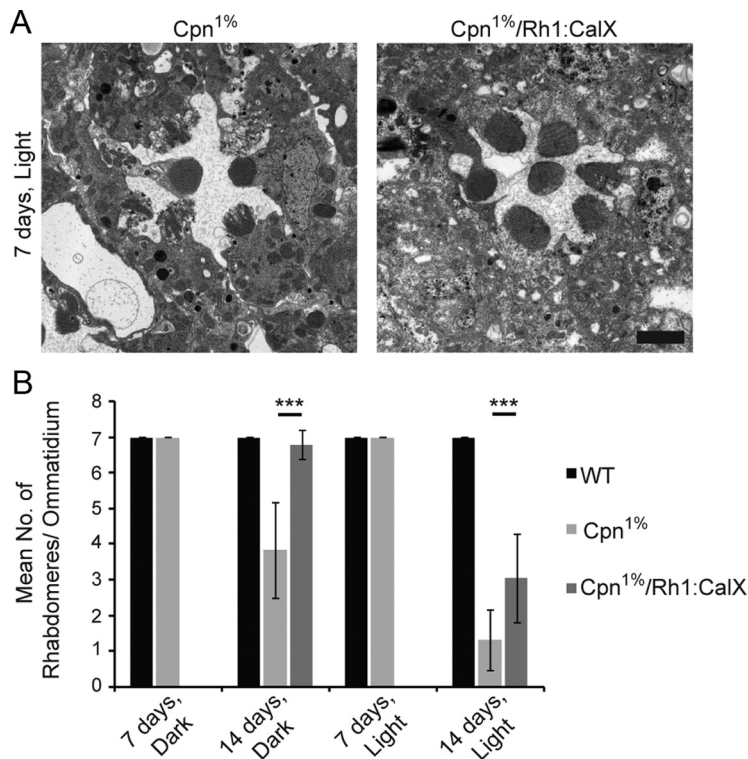


Figure 7. Overexpressing the Na⁺-Ca²⁺ exchanger CalX rescues the light-induced photoreceptor degeneration of the Cpn^{1%}. **A**, Overexpression of CalX on Cpn^{1%} background partially rescues the degenerative phenotype at age 7 d. Scale bar, 2 μ m. **B**, Quantification of the mean number of rhabdomeres per ommatidium (mean \pm SEM, $n \geq 50$ ommatidia, $N = 2$ flies, *** $p < 0.005$).

Cellular Ca²⁺ dynamics following signal-induced Ca²⁺ influx is affected by Cpn

The high quantity of Cpn, the protein's strategic localization along the rhabdomere, its hydrophobic nature, its *in vitro* Ca²⁺-binding properties (Martin et al., 1993), and the results presented above (Figs. 4–7) suggest that Cpn plays an important role in cellular Ca²⁺ homeostasis. To directly measure the effects of Cpn on cellular Ca²⁺ dynamics following signal-induced Ca²⁺ influx, we applied Ca²⁺ imaging in photoreceptor and in HEK cells heterologously expressing Cpn.

Ca²⁺ measurements in photoreceptor cells

Cellular measurements of Ca²⁺ using fluorescent Ca²⁺ indicators in *Drosophila* photoreceptors require extreme nonphysiological intense illumination, resulting in simultaneous activation of highly abundant Ca²⁺-permeable TRP and TRP-like channels. Under this intense illumination, which induces massive Ca²⁺ influx into the rhabdomere, a diffusion of Ca²⁺ from the rhabdomere to the cell body was observed (Peretz et al., 1994a; Hardie, 1996; Oberwinkler and Stavenga, 2000b).

Under these conditions, we compared the kinetics of cellular Ca²⁺ elevation in WT and Cpn^{1%} flies using the fluorescence of a low-affinity Ca²⁺ indicator and reduced extracellular [Ca²⁺] to prevent saturation of the Ca²⁺ indicator (see Materials and Methods).

Figure 8A shows the light-induced changes of cellular Ca²⁺ as a function of time (Fig. 8Aa) in newly eclosed dark-raised WT and Cpn^{1%} flies, which showed virtually normal rhabdomeres (Fig. 3A,B). In WT flies, the rise in intracellular Ca²⁺ was slow, reaching 95% of maximum amplitude after 381 ± 42 ms (Fig. 8Aa,Ab). Strikingly, in the Cpn^{1%} flies, the rise time of the increase in cellular Ca²⁺ was fast, reaching 95% maximum ampli-

tude after 22 ms (Fig. 8Aa,Ab). Importantly, there was a marked and significant difference in the rise time of the increase in cellular Ca²⁺ between WT and Cpn^{1%} flies ($p < 0.005$) and in the Ca²⁺ level measured at 22 ms after light onset ($p < 0.05$). However, there was no significant difference in the steady-state Ca²⁺ level between WT and Cpn^{1%} flies ($p \gg 0.05$), suggesting that Cpn functions as an immobile Ca²⁺ buffer (see Discussion) (Schwaller, 2010).

Single-cell imaging clearly showed a gradual increase in photoreceptor Ca²⁺ as a function of time during illumination in WT flies (Fig. 8B, left). In contrast, in Cpn^{1%} flies, the fluorescent intensity reached a maximal level within the first frame (Fig. 8B, right). Thus, Ca²⁺ measurements in Cpn^{1%} flies indicate that upon intense illumination, in the absence of Cpn, cellular Ca²⁺ increased much faster than it does in WT flies. These results demonstrate that in WT flies, the presence of Cpn prevents a fast increase in cellular Ca²⁺ despite the massive light-induced Ca²⁺ influx via fast opening of TRP and TRP-like channels (Peretz et al., 1994a). Altogether, the data suggest that Cpn regulates cellular Ca²⁺ dynamics in a manner expected from an immobile Ca²⁺ buffer (see Discussion).

Ca²⁺ measurements in HEK293 cells expressing Cpn

To test whether Cpn affects cellular Ca²⁺ dynamics in isolation, we heterologously expressed Cpn in HEK293 cells. Cpn was uniformly expressed throughout the cytoplasm of the cells (Fig. 8Ca). To induce cellular Ca²⁺ elevation upon signaling, we co-expressed Cpn together with the Ca²⁺-permeable TRPV1 channel, which can be robustly activated by application of capsaicin (Caterina et al., 1997). Using the fluorescence of the Fura-2 indicator, measurements were made of intracellular [Ca²⁺] as a function of time following application of capsaicin (Fig. 8Cb). As a control, we repeated the experiments in HEK293 cells expressing only TRPV1. Strikingly, a significantly larger increase in cellular [Ca²⁺] was observed in cells expressing only TRPV1, as opposed to cells expressing both TRPV1 and Cpn (Fig. 8Cb, upper trace vs lower trace, $p < 0.01$ for the steady-state [Ca²⁺]). Since Cpn was uniformly expressed throughout the cytoplasm of the cells (Fig. 8Ca), and was not localized to a specific cellular area, we assume that the proteins localizing Cpn to its defined cytoplasmic area in photoreceptor cells are absent in HEK cells. Unlike the situation in photoreceptor cells, the expressed Cpn in HEK cells thus functions as a mobile Ca²⁺ buffer (see Discussion).

This result directly indicates that Cpn is an efficient Ca²⁺ buffer, both necessary and sufficient for elevating the Ca²⁺-buffering capacity of cells.

Discussion

Cpn's role in Ca²⁺ homeostasis is essential to prevent light-induced photoreceptor degeneration

In many sensory neurons, the entire transduction machinery is housed in a specialized cellular compartment (Avidor-Reiss et al.,

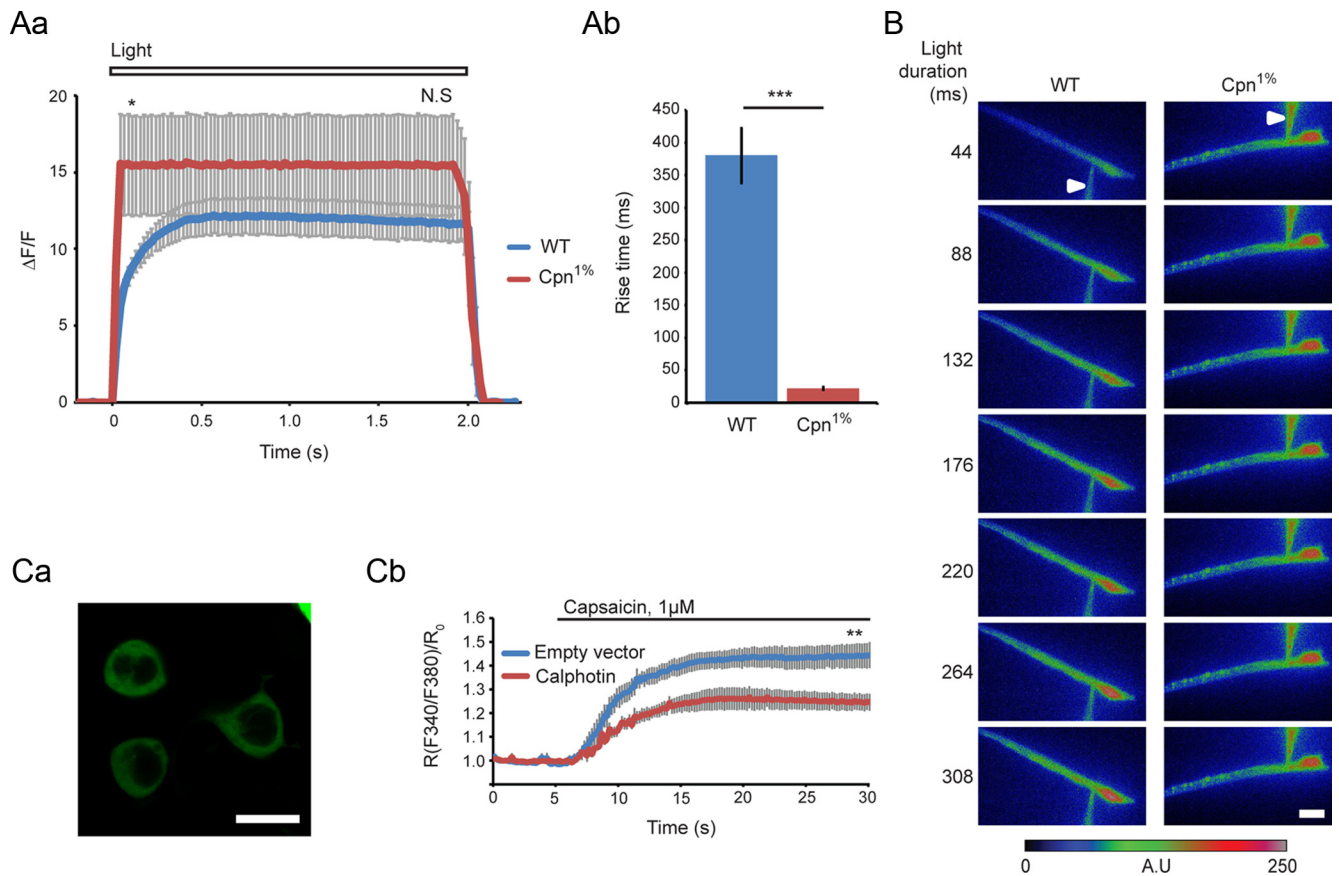


Figure 8. Measurements of intracellular Ca^{2+} in photoreceptors lacking Cpn and in HEK cells overexpressing Cpn. **A**, Cellular Ca^{2+} dynamics following signal-induced Ca^{2+} influx in WT and Cpn^{1%} flies using the fluorescent Ca^{2+} indicators, calcium green 5N while the extracellular $[\text{Ca}^{2+}]$ was 0.4 mM. A comparison of the light-induced changes of cellular Ca^{2+} as a function of time between WT and Cpn^{1%} flies. **Aa**, Measurements of the light-induced $[\text{Ca}^{2+}]$ increase in WT and Cpn^{1%} flies (averaged, $n = 10$). When comparing the light-induced fluorescent increase between WT and Cpn^{1%}, a significant difference was observed at the initial level of the fluorescence ($*p < 0.05$) but not during the steady state (N.S. > 0.05). **Ab**, Time to 95% of maximal fluorescence intensity. Histogram comparing the individual traces of **Aa** (mean \pm SEM, $***p < 0.005$). **B**, Time series of photoreceptor images of WT and Cpn^{1%} flies showing the fluorescence of the Ca^{2+} indicator during light stimulation. Raw intensity images are plotted by using false-color coding. Arrowheads indicate the pipette. Scale bar, 10 μm . **C**, Heterologous expression of Cpn in HEK293 cells. **Ca**, Confocal image showing cytosolic localization of GFP-tagged Cpn. Scale bar, 10 μm . **Cb**, Ca^{2+} imaging using fluorescent ratio of the Fura-2 calcium indicator as a function of time ($n = 7$ for each dataset, mean \pm SEM, $**p < 0.01$ for the steady-state phase). Cells were cotransfected with TRPV1 and Ca^{2+} influx was induced by application of capsaisin (1 μM).

2004). The process of compartmentalization requires localization of building-block proteins between the cell body and the signaling compartment. The exchange of ions and proteins between these two compartments is highly regulated by the properties of these building blocks.

In fly photoreceptors, the signaling machinery resides inside microvilli. These microvilli, like microvilli in other microvilli-containing cells, are connected directly to the cell body (for review, see Hardie and Raghu, 2001; Katz and Minke, 2009). This structure makes the regulation of ion exchange between the two compartments particularly challenging and largely unknown. The localization of a large number of Ca^{2+} -permeable TRP channels in the microvilli and the observed large increase of microvillar Ca^{2+} upon illumination constitute a high risk of Ca^{2+} overload in the cell body, where abnormally elevated $[\text{Ca}^{2+}]$ activates powerful mechanisms of cell death (for review, see Zhivotovsky and Orrenius, 2011).

In this study we used two independent experiments to demonstrate that Cpn is essential for Ca^{2+} homeostasis: (1) measurements of pigment granule migration and (2) the appearance of dark bumps following artificial increase of cell-body Ca^{2+} . In the first experiment, dim red light was used during the preparation of dark-raised flies for EM analysis of pigment granule localization. Because of the extreme sensitivity of pigment granule migration to light-induced Ca^{2+} elevation (Satoh et al., 2008), the

dim red light was selected to prevent pigment granule movement in WT flies (see Materials and Methods). Strikingly, under the same conditions, this dim red light caused sufficient elevation of cellular Ca^{2+} to induce pigment granule movement to the light-adapted position in dark-adapted Cpn^{90%} flies (Fig. 4), presumably due to inefficient Ca^{2+} extrusion from the photoreceptors of Cpn^{90%} flies. In the second experiment, artificially elevated $[\text{Ca}^{2+}]$ in the cell body caused an increase in rhabdomeral Ca^{2+} , which was larger in the Cpn^{90%} flies than in WT flies due to an enhanced Ca^{2+} diffusion from the cell body to the rhabdomere in dark-adapted Cpn-RNAi flies.

The use of Cpn^{90%} and Cpn^{50%} flies revealed that impaired Ca^{2+} homeostasis exists without any sign of photoreceptor degeneration, thus precluding the possibility that impaired morphology is the cause of impaired Ca^{2+} homeostasis.

Cpn functions as an immobile Ca^{2+} buffer

Until now, the term Ca^{2+} buffer has been applied only to a small subset of cytosolic proteins of the EF family. Often, a distinction is made between mobile and immobile buffers (Zhou and Neher, 1993). The latter are defined as molecules capable of binding cytosolic Ca^{2+} even if the cytosol is washed by a patched pipette. Yet, aside from these features, very little is known about the molecular identity of immobile Ca^{2+} buffers (Schwaller, 2010).

The restricted rhabdomeric volume contains large amounts of both Ca²⁺-permeable channels, TRP and TRP-like (Huber et al., 1996; Niemeyer et al., 1996), and the Ca²⁺ extrusion protein, CalX (Oberwinkler and Stavenga, 2000b; Wang et al., 2005), thus making the control of [Ca²⁺] in the rhabdomere very efficient (Oberwinkler and Stavenga, 2000a). Ca²⁺ influx initially leads to a high rhabdomeral [Ca²⁺]. Powerful mechanisms are then quickly activated to reduce rhabdomeral Ca²⁺ during light. These mechanisms include a fast reduction in Ca²⁺ influx by light adaptation and by divalent open-channel block of the TRP and TRP-like channels (Parnas et al., 2007), together with activation of the Na⁺–Ca²⁺ exchanger (Wang et al., 2005). It was previously shown in *Calliphora* flies that the increase in both cell-body and rhabdomeral Ca²⁺ lag behind the full opening of the light-sensitive and Ca²⁺-permeable channels. This puzzling observation was explained by assuming that Ca²⁺ influx is buffered (Oberwinkler and Stavenga, 1998). To directly measure the effects of Cpn on cellular Ca²⁺ dynamics following signal-induced Ca²⁺ influx, we applied Ca²⁺ imaging in photoreceptor cells and in HEK cells heterologously expressing Cpn. We showed that a major role of Cpn is to slow down the increase in cellular Ca²⁺ (Fig. 8A, B), a typical function of a Ca²⁺ buffer. The specific cellular localization of Cpn (Fig. 1B), which was not affected by washing the cytosol with the whole-cell patch-clamp pipette (Fig. 8B) indicates that Cpn is an immobile Ca²⁺ buffer (Schwaller, 2010). Cpn was also shown to affect cellular Ca²⁺ dynamics in isolation by heterologous expression in HEK293 cells. Since Cpn was uniformly expressed throughout the cytoplasm of the cells (Fig. 8Ca) and was not localized to a specific cellular area, we assume that the proteins localizing Cpn to its defined cytoplasmic area in photoreceptor cells are absent in HEK cells. Unlike the situation in photoreceptor cells, in HEK cells the expressed Cpn thus functions as a mobile Ca²⁺ buffer. Mobile buffers bind Ca²⁺ and then, by buffered diffusion, spread the Ca²⁺ deeper into the cytoplasm. Ca²⁺-bound mobile buffers are replaced by Ca²⁺-free molecules and thus will reduce [Ca²⁺] until the total buffer pool is saturated (Parekh, 2008). The observation of a significantly lower steady-state Ca²⁺ level in HEK cells expressing Cpn relative to control suggest that saturation of the buffer (i.e., Cpn) was not obtained. This is because Ca²⁺ extrusion mechanisms must be activated by the Ca²⁺ influx.

In summary, Cpn regulates cellular Ca²⁺ dynamics in photoreceptor cells in a manner expected from an immobile Ca²⁺ buffer.

Photoreceptor mechanisms underlying Ca²⁺ homeostasis

The specific localization of Cpn at the boundary between the rhabdomere and cell body reduces Ca²⁺ diffusion to the cell body during light. The cell body does not have the wherewithal to handle massive Ca²⁺ diffusion because the major Ca²⁺ extrusion protein CalX is virtually absent in this portion of the photoreceptor (Wang et al., 2005). Hence, continuous Ca²⁺ diffusion to this compartment leads to Ca²⁺ overload and cell degeneration (Figs. 2, 3).

Three major mechanisms prevent Ca²⁺ overload in the cell body during prolonged lights: (1) the controlled Ca²⁺ influx via the light-sensitive channels (Parnas et al., 2007), (2) Ca²⁺ extrusion by CalX (Wang et al., 2005), and (3) limited Ca²⁺ diffusion from the rhabdomere to the cell body by binding of Ca²⁺ to Cpn. All three mechanisms must operate to prevent Ca²⁺ overload in the cell body. This was demonstrated by mutations that eliminate one of the three mechanisms, leading to retinal degeneration despite the proper operation of the other two. The demonstrations included constitutive unregulated activity of TRP channels

(Yoon et al., 2000), elimination of CalX (Wang et al., 2005), and elimination of Cpn (Fig. 3). The fact that overexpression of CalX partially rescues the degeneration induced by malfunction of each of the other two mechanisms indicates that Ca²⁺ overload is the common denominator underlying degeneration in these cases.

References

- Abramoff MD, Magalhães PJ, Ram SJ (2004) Image processing with ImageJ. *Biophotonics International* 11:36–42.
- Augustine GJ, Neher E (1992) Neuronal Ca²⁺ signalling takes the local route. *Curr Opin Neurobiol* 2:302–307.
- Avidor-Reiss T, Maer AM, Koundakjian E, Polyanovsky A, Keil T, Subramaniam S, Zuker CS (2004) Decoding cilia function: defining specialized genes required for compartmentalized cilia biogenesis. *Cell* 117:527–539.
- Ballinger DG, Xue N, Harshman KD (1993) A *Drosophila* photoreceptor cell-specific protein, calphotin, binds calcium and contains a leucine zipper. *Proc Natl Acad Sci U S A* 90:1536–1540.
- Caterina MJ, Schumacher MA, Tominaga M, Rosen TA, Levine JD, Julius D (1997) The capsaicin receptor: a heat-activated ion channel in the pain pathway. *Nature* 389:816–824.
- Chang HY, Ready DF (2000) Rescue of photoreceptor degeneration in rhodopsin-null *Drosophila* mutants by activated Rac1. *Science* 290:1978–1980.
- Chorna-Ornan I, Tzarfaty V, Ankri-Eliashoo G, Joel-Almagor T, Meyer NE, Huber A, Payre F, Minke B (2005) Light-regulated interaction of Dmoeosin with TRP and TRPL channels is required for maintenance of photoreceptors. *J Cell Biol* 171:143–152.
- Cosens D, Perry MM (1972) The fine structure of the eye of a visual mutant, A-type of *Drosophila melanogaster*. *J Insect Physiol* 18:1773–1786.
- Elia N, Frechter S, Gedi Y, Minke B, Selinger Z (2005) Excess of G_β over G_{αq} *in vivo* prevents dark, spontaneous activity of *Drosophila* photoreceptors. *J Cell Biol* 171:517–526.
- Endo H, Persson P, Watanabe T (2000) Molecular cloning of the crustacean DD4 cDNA encoding a Ca(2+)-binding protein. *Biochem Biophys Res Commun* 276:286–291.
- Franceschini N, Kirschfeld K (1971a) In vivo optical study of photoreceptor elements in the compound eye of *Drosophila* (in French). *Kybernetik* 8:1–13.
- Franceschini N, Kirschfeld K (1971b) Pseudopupil phenomena in the compound eye of *Drosophila* (in French). *Kybernetik* 9:159–182.
- Franceschini N, Kirschfeld K (1976) Le contrôle automatique du flux lumineux dans l'oeil composé des diptères. *Biol Cybern* 21:181–203.
- Gu Y, Oberwinkler J, Postma M, Hardie RC (2005) Mechanisms of light adaptation in *Drosophila* photoreceptors. *Curr Biol* 15:1228–1234.
- Hardie RC (1995) Photolysis of caged Ca²⁺ facilitates and inactivates but does not directly excite light-sensitive channels in *Drosophila* photoreceptors. *J Neurosci* 15:889–902.
- Hardie RC (1996) INDO-1 measurements of absolute resting and light-induced Ca²⁺ concentration in *Drosophila* photoreceptors. *J Neurosci* 16:2924–2933.
- Hardie RC, Minke B (1992) The *trp* gene is essential for a light-activated Ca²⁺ channel in *Drosophila* photoreceptors. *Neuron* 8:643–651.
- Hardie RC, Raghu P (2001) Visual transduction in *Drosophila*. *Nature* 413:186–193.
- Huber A, Sander P, Gobert A, Böhner M, Hermann R, Paulsen R (1996) The transient receptor potential protein (Trp), a putative store-operated Ca²⁺ channel essential for phosphoinositide-mediated photoreception, forms a signaling complex with NorpA, InaC and InaD. *EMBO J* 15:7036–7045.
- Iakhine R, Chorna-Ornan I, Zars T, Elia N, Cheng Y, Selinger Z, Minke B, Hyde DR (2004) Novel dominant rhodopsin mutation triggers two mechanisms of retinal degeneration and photoreceptor desensitization. *J Neurosci* 24:2516–2526.
- Katz B, Minke B (2009) *Drosophila* photoreceptors and signaling mechanisms. *Front Cell Neurosci* 3:2.
- Katz B, Minke B (2012) Phospholipase C-mediated suppression of dark noise enables single-photon detection in *Drosophila* photoreceptors. *J Neurosci* 32:2722–2733.
- Kirschfeld K, Vogt K (1980) Calcium ions and pigment migration in fly photoreceptors. *Naturwissenschaften* 67:516–517.
- Koch C, Zador A (1993) The function of dendritic spines: devices subserv-

- ing biochemical rather than electrical compartmentalization. *J Neurosci* 13:413–422.
- Lee YS, Carthew RW (2003) Making a better RNAi vector for *Drosophila*: use of intron spacers. *Methods* 30:322–329.
- Lenzi D, Roberts WM (1994) Calcium signalling in hair cells: multiple roles in a compact cell. *Curr Opin Neurobiol* 4:496–502.
- Lo MV, Pak WL (1981) Light-induced pigment granule migration in the reticular cells of *Drosophila melanogaster*. Comparison of wild type with ERG-defective mutants. *J Gen Physiol* 77:155–175.
- Martin JH, Benzer S, Rudnicka M, Miller CA (1993) Calphotin: a *Drosophila* photoreceptor cell calcium-binding protein. *Proc Natl Acad Sci U S A* 90:1531–1535.
- Niemeyer BA, Suzuki E, Scott K, Jalink K, Zuker CS (1996) The *Drosophila* light-activated conductance is composed of the two channels TRP and TRPL. *Cell* 85:651–659.
- Oberwinkler J, Stavenga DG (1998) Light dependence of calcium and membrane potential measured in blowfly photoreceptors *in vivo*. *J Gen Physiol* 112:113–124.
- Oberwinkler J, Stavenga DG (2000a) Calcium transients in the rhabdomeres of dark- and light-adapted fly photoreceptor cells. *J Neurosci* 20:1701–1709.
- Oberwinkler J, Stavenga DG (2000b) Calcium imaging demonstrates colocalization of calcium influx and extrusion in fly photoreceptors. *Proc Natl Acad Sci U S A* 97:8578–8583.
- Parekh AB (2008) Ca^{2+} microdomains near plasma membrane Ca^{2+} channels: impact on cell function. *J Physiol* 586:3043–3054.
- Parnas M, Katz B, Minke B (2007) Open channel block by Ca^{2+} underlies the voltage dependence of *Drosophila* TRPL channel. *J Gen Physiol* 129:17–28.
- Parnas M, Peters M, Dadon D, Lev S, Vertkin I, Slutsky I, Minke B (2009) Carvacrol is a novel inhibitor of *Drosophila* TRPL and mammalian TRPM7 channels. *Cell Calcium* 45:300–309.
- Peretz A, Suss-Toby E, Rom-Glas A, Arnon A, Payne R, Minke B (1994a) The light response of *Drosophila* photoreceptors is accompanied by an increase in cellular calcium: effects of specific mutations. *Neuron* 12:1257–1267.
- Peretz A, Sandler C, Kirschfeld K, Hardie RC, Minke B (1994b) Genetic dissection of light-induced Ca^{2+} influx into *Drosophila* photoreceptors. *J Gen Physiol* 104:1057–1077.
- Satoh AK, Li BX, Xia H, Ready DF (2008) Calcium-activated myosin V closes the *Drosophila* pupil. *Curr Biol* 18:951–955.
- Schwaller B (2010) Cytosolic Ca^{2+} buffers. *Cold Spring Harb Perspect Biol* 2:a004051.
- Tsunoda S, Sierralta J, Sun Y, Bodner R, Suzuki E, Becker A, Socolich M, Zuker CS (1997) A multivalent PDZ-domain protein assembles signalling complexes in a G-protein-coupled cascade. *Nature* 388:243–249.
- Wang T, Xu H, Oberwinkler J, Gu Y, Hardie RC, Montell C (2005) Light activation, adaptation, and cell survival functions of the $\text{Na}^+/\text{Ca}^{2+}$ exchanger CalX. *Neuron* 45:367–378.
- Yang Y, Ballinger D (1994) Mutations in *calphotin*, the gene encoding a *Drosophila* photoreceptor cell-specific calcium-binding protein, reveal roles in cellular morphogenesis and survival. *Genetics* 138:413–421.
- Yoon J, Cohen Ben-Ami HC, Hong YS, Park S, Strong LL, Bowman J, Geng C, Baek K, Minke B, Pak WL (2000) Novel mechanism of massive photoreceptor degeneration caused by mutations in the *trp* gene of *Drosophila*. *J Neurosci* 20:649–659.
- Zhivotovsky B, Orrenius S (2011) Calcium and cell death mechanisms: a perspective from the cell death community. *Cell Calcium* 50:211–221.
- Zhou Z, Neher E (1993) Mobile and immobile calcium buffers in bovine adrenal chromaffin cells. *J Physiol* 469:245–273.